MINERALOGICAL MAGAZINE

VOLUME 51 NUMBER 360 JUNE 1987

The 1875 eruption of Askja volcano, Iceland: combined fractional crystallization and selective contamination in the generation of rhyolitic magma

R. MACDONALD

Department of Environmental Science, University of Lancaster, Lancaster LA1 4YQ, U.K.

R. S. J. SPARKS

Department of Earth Sciences, University of Cambridge, Cambridge CB2 3EQ, U.K.

H. SIGURDSSON

Graduate School of Oceanography, University of Rhode Island, Narragansett, RI 02882, U.S.A.

D. P. MATTEY, D. W. MCGARVIE

Department of Earth Sciences, The Open University, Milton Keynes MK7 6AA, U.K.

AND

R. L. SMITH

U.S. Geological Survey, 2943C Fulton Avenue, Sacramento, CA 95821, U.S.A.

Abstract

Major and trace element and Sr, Nd and O isotopic data are presented for ferrobasalts, icelandites, rhyolites, mixed pumices and silicic xenoliths of the 1875 eruption of Askja. Trace element modelling and Sr and Nd data largely confirm previous major element calculations that fractional crystallization was dominant in the generation of the basalt–ferrobasalt–icelandite–rhyolite suite. Relative enrichment in Rb (and Th and U?), depletion in Cs, and low values of $\delta^{18}O/^{16}O$, in the rhyolites are not explained by this mechanism alone. The silicic magmas were selectively contaminated by diffusion from partially molten granitic wall rocks, now found as xenoliths in the eruptive products, the process being particularly marked by lower $\delta^{18}O$ and Cs/Rb ratios in the rhyolites than in the associated basalts. This is the first record of a combined fractional crystallization-selective contamination process in an Icelandic silicic complex.

KEYWORDS: volcanoes, rhyolitic magma, isotope data, Askja volcano, Iceland.

Introduction

IN the spectrum of silicic volcanism (Smith, 1979), Askja is a small magnitude basalt–rhyolite system. Magma mixing phenomena are often common in such systems. Mixing causes compositional variation among the magmatic products and perhaps acts as an eruptive trigger (Sparks *et al.*, 1977). The

Mineralogical Magazine, June 1987, Vol. 51, pp. 183–202
© *Copyright the Mineralogical Society*

Table 1. Trace element data for rocks of 1875 Askja eruption.

	← RHYOLITIC PUMICE →										BULK ASH
Unit	Early obs.flow	Layer B	Layer C2			Layer C1			Layer D			Layer C
Spec no.(As-)	16	114(a)	103	104	108	105	106	107	100	101	102	2
(ppm)												
Ba	416	358	405	389	371	384	343	365	388	383	390	364
Co	6.8	4.1	6.9	4.1	4.1	3.9	4.5	4.2	4.8	7.3	4.9	10.1
Cr	8.4	<4	<3	<9	3.9	<3	<9	<3	3.6	<10	<8	4.6
Cs	0.4	0.7	0.6	0.7	0.6	0.7	0.5	0.6	0.6	0.6	0.6	0.5
Hf	11.2	9.5	9.5	9.6	9.6	9.4	9.4	9.4	9.3	9.0	8.8	8.6
Nb	37	39	36	37	37	36	37	39	34	31	34	30
Pb	15	9	8	14	24	10	5	13	21	17	14	18
Rb	54	66	58	60	66	58	65	58	65	58	65	48
Sc	12.8	11.30	13.80	11.30	10.40	11.00	11.50	11.30	11.80	14.20	11.40	15.30
Sr	121	117	128	117	112	129	116	122	129	140	125	130
Ta	2.60	2.62	2.69	2.55	2.67	2.58	2.53	2.59	2.54	2.50	2.32	2.36
Th	6.5	7.5	6.9	7.2	7.6	7.2	7.2	7.3	7.3	6.9	6.9	6.3
U	2.0	2.0	1.8	1.9	2.1	2.2	2.3	1.9	1.9	2.2	2.2	1.6
Y	70	67	64	69	69	71	67	66	69	64	60	60
Zn	72	67	79	78	74	74	70	79	72	85	69	78
Zr	428	362	327	348	373	343	341	351	351	315	328	298
La	44	42	39	40	41	40	41	41	40	40	39	36
Ce	87	82	79	80	81	78	79	79	80	78	76	71
Nd	39	39	39	43	39	39	41	37	38	37	36	31
Sm	10.5	7.9	9.7	8.5	7.7	10.9	8.6	7.6	10.4	10.6	9.7	8.9
Eu	2.11	1.98	2.06	1.89	1.91	1.90	1.93	1.92	1.95	2.05	1.84	1.84
Gd	10.9	10.4	9.2	10.4	10.1	8.5	9.5	10.4	10.1	9.9	9.5	8.4
Tb	1.48	1.50	1.63	1.54	1.47	1.40	1.52	1.48	1.44	1.49	1.37	1.34
Tm	0.91	0.92	0.81	0.88	0.86	0.82	0.74	0.78	0.85	0.68	0.93	0.75
Yb	6.7	6.5	6.4	6.4	6.5	6.3	6.1	6.3	6.4	6.4	6.0	5.8
Lu	0.94	0.93	0.89	0.90	0.91	0.87	0.88	0.90	0.88	0.89	0.84	0.81

	← MIXED PUMICE →				← ICELANDITE →				← BASALTS →			
	71(c)	414	28B	229	28A	12	71g	RLS	56	256	265	266
Ba	242	239	308	379	-	255	156	-	163	184	185	184
Co	15.4	31.8	24.5	8.4	17.5	20.1	18.0	17.3	47.1	48.2	48.2	46.5
Cr	24.0	29.0	19.2	<3	<10	2.7	<6.0	<20	35.4	23.4	25.8	27.6
Cs	0.5	0.3	0.5	0.5	0.6	0.5	0.4	<0.6	<0.8	0.2	<0.8	0.2
Hf	7.3	6.0	6.6	8.7	7.7	6.9	6.7	6.7	4.4	4.4	4.5	4.4
Nb	32	26	-	38	-	30	39	29	24	25	23	22
Pb	16	9	15	17	-	7	19	-	1	10	8	12
Rb	41	27	31	58	-	35	31	37	8	12	12	9
Sc	19.60	30.80	25.70	15.00	24.00	25.70	24.00	23.80	41.30	42.50	43.10	41.60
Sr	137	148	145	137	-	176	166	-	171	174	177	166
Ta	2.21	1.81	1.96	2.47	2.28	2.19	2.21	2.08	1.54	1.40	1.44	1.40
Th	5.4	3.7	4.6	6.5	5.1	4.6	4.5	4.4	1.5	1.5	1.6	1.5
U	1.6	1.4	1.0	1.7	1.5	1.4	0.9	0.9	<2.0	0.7	0.7	<2
Y	49	63	41	67	-	51	55	-	21	38	38	41
Zn	96	93	98	94	-	122	124	-	129	96	109	106
Zr	277	204	221	320	-	236	240	-	139	132	129	114
La	31	25	27	38	37	31	32	31	17	17	17	17
Ce	61	49	54	75	70	64	65	63	34	37	36	36
Nd	34	30	35	40	47	42	35	52	26	26	28	24
Sm	6.9	6.1	6.4	7.7	8.5	8.0	8.2	7.7	5.4	5.5	5.6	5.5
Eu	1.75	1.76	1.71	2.06	2.43	2.33	2.34	2.28	1.83	1.90	1.96	1.88
Gd	7.9	8.0	7.9	9.7	11.8	10.1	10.3	8.5	6.7	7.0	7.8	7.0
Tb	1.39	1.17	1.35	1.49	1.52	1.45	1.46	1.62	1.18	1.15	1.22	1.13
Tm	0.73	0.69	0.77	0.89	0.68	0.99	0.85	0.85	0.68	0.55	0.58	0.67
Yb	5.4	4.8	5.1	6.3	6.4	5.9	5.8	5.8	4.3	4.6	4.6	4.5
Lu	0.79	0.71	0.72	0.89	0.90	0.83	0.86	0.82	0.63	0.67	0.68	0.67

Table 1 continued

	← GROUP I XENOLITHS →							← GROUP II XENOLITHS →				
	411	15	400	275	415	412A	413	401	402	410	270	30
Ba	431	474	393	367	486	397	-	410	318	295	478	432
Co	5.0	4.2	5.2	4.4	4.4	6.0	17.5	4.2	0.7	4.3	0.3	4.4
Cr	4.7	<8	<8	1.3	2.2	<8	<4	<7	<6	6.3	2.4	8.1
Cs	0.5	0.5	0.6	0.3	0.4	0.5	0.5	0.4	0.3	0.1	0.2	<0.4
Hf	11.7	11.2	12.3	12.0	11.5	10.7	7.0	11.8	11.7	11.0	12.4	10.6
Nb	41	39	37	36	41	39	30	39	48	55	59	45
Pb	18	10	24	18	26	13	-	25	19	21	28	<1
Rb	53	58	52	50	58	59	37	58	54	56	55	46
Sc	10.90	9.91	11.50	11.40	10.30	11.90	24.40	10.10	2.28	5.09	2.31	5.30
Sr	111	111	109	123	111	129	-	122	69	23	90	110
Ta	3.02	2.85	2.87	2.81	3.00	2.79	2.27	2.96	3.97	4.11	4.43	3.93
Th	7.3	7.1	6.4	6.4	6.8	6.6	4.6	7.4	7.5	7.9	8.3	7.3
U	2.7	1.9	2.0	1.9	2.0	2.0	1.5	2.1	2.0	2.9	2.5	2.0
Y	68	53	69	75	65	75	-	69	108	115	127	87
Zn	57	57	56	33	53	63	-	62	97	21	84	66
Zr	419	430	480	494	439	421	-	450	346	347	374	325
La	40	37	43	45	40	40	32	42	41	56	63	52
Ce	80	74	84	89	80	79	66	84	93	114	131	108
Nd	37	37	43	44	38	41	41	43	54	60	67	55
Sm	8.0	7.5	8.0	8.4	8.1	8.1	8.0	8.2	11.6	12.7	14.3	11.5
Eu	1.95	1.89	2.05	2.12	2.04	2.16	2.35	2.00	2.16	2.64	3.02	2.41
Gd	9.1	9.1	9.4	10.7	11.0	10.2	9.9	9.7	16.6	16.5	18.4	14.4
Tb	1.60	1.41	1.54	1.62	1.60	1.56	1.59	1.54	2.67	2.55	2.89	2.26
Tm	0.84	0.80	0.88	0.88	0.94	0.90	0.87	0.97	1.53	1.58	1.80	1.41
Yb	6.6	6.1	6.6	6.8	6.4	6.4	6.0	6.7	10.4	10.6	12.5	9.4
Lu	0.94	0.88	0.96	0.97	0.92	0.92	0.84	0.96	1.44	1.43	1.70	1.31

1875 eruption of Askja is perhaps the best documented of all Icelandic basalt–rhyolite mixed eruptions and provides a good case for investigating the geochemical relationships among magma types. Sigurdsson and Sparks (1981) presented detailed mineralogical and major element analytical results on the products of the 1875 eruption and suggested that the series evolved by a complex combination of fractional crystallization, magma mixing, and melting of granitic wall rocks.

This study was undertaken to provide a comprehensive body of trace element data for a well documented suite of silicic rocks in Iceland, and to test and possibly to refine the petrogenetic models of Sigurdsson and Sparks (1981). An important conclusion is that the 1875 rhyolites were selectively contaminated in certain alkali elements by diffusion from partially melted wall rocks. While this mechanism is being increasingly recognized in continental suites (Carlson *et al.*, 1981; Thompson *et al.*, 1982; Norry and Fitton, 1983; Thirlwall and Jones, 1983; Cox and Hawkesworth, 1985), this is apparently the first record of its operation in an oceanic complex.

The general volcanological and petrological background to the 1875 eruption is given by Sigvaldason (1979), Sparks *et al.* (1981) and Sigurdsson and Sparks (1978, 1981). The 1875 ejecta consist of at least 0.2 km^3 of crystal-poor ($\sim 1\%$) rhyolitic pumice and ash. Numerous inclusions and streaks of tholeiitic basalt, ferrobasalt and icelandite occur within individual pumice clasts. Textural evidence indicates that these materials were mixed as magma into the rhyolite either shortly before or during eruption.

A suite of partially fused, leucocratic xenoliths was also erupted. The texture of the xenoliths (Sigurdsson and Sparks, 1981) shows very intimate interpenetration of glass (partial melt) and broken-down mineral residue. Fingerprint and sieve textures are typical, suggesting inefficient separation of partial melt and residue. In addition, a contemporaneous fissure eruption of 0.3 km^3 of ferrobasalt occurred at Sveinagja, 70 km north of Askja, and is considered to represent lateral drainage of magma from the Askja reservoir.

Analytical methods

Trace element data for Askja rocks are given in Table 1. Ba, Pb, Rb, Sr, Y, Zn and Zr were determined by XRF at the University of Lancaster, using a Philips 1400 spectrometer. Other elements were analysed by INAA at the U.S. Geological

Survey in Reston. Estimates of precision for both techniques are as given by Bacon *et al.* (1981, Table 1). Nb was determined spectrophotometrically, with an estimated precision of 10% (1σ); the results were also checked independently by XRF. Major element analyses of specimens (As-) 114, 103, 105, 100, 28B, 229, 28A, 12, 15, 56, 400, 275, 415, 412A, 401 and 30 may be found in Sigurdsson and Sparks (1981). No major element data are available for (As-) 108, 71g, RLS and 413. Analyses of remaining specimens are given in Table 2.

The analysed specimens comprise rhyolite pumices, bulk ash samples, obsidian flows, mixed pumices, icelandite inclusions, ferrobasalts of the Sveinagja fissure eruption and various leucocratic xenoliths. The suite of samples selected for analysis are all very fresh rocks. However the xenoliths show extensive hydrothermal alteration; the chemical effects of this alteration are discussed below. An important constraint on petrogenetic discussion using the trace element data is that it is impossible to completely separate the rhyolitic glass from the more mafic materials found as components of the pumices and from the glass formed by fusion of the xenoliths.

Oxygen isotope analyses were performed by reaction with ClF_3 at 625 °C using essentially the same procedure as that described by Borthwick and Harmon (1982). Measurements are precise to within $\pm 0.1‰$ (based on replicate analyses) and a

Table 2. Major element analyses of Askja rocks.

ERUPTIVE UNIT	Early obsidian flow	Layer C2	Layer C1		Layer D		Bulk ash, Layer C	Mixed pumice	
Sample No.(AS-)	16	104	106	107	101	102	2	71(c)	414
SiO_2	70.52	73.16	72.34	73.16	70.14	72.63	68.87	65.04	58.25
Al_2O_3	12.95	12.50	12.65	12.49	12.51	12.87	12.57	14.12	12.84
Fe_2O_3	1.20	-	-	-	-	-	-	-	-
FeO	3.20	3.83*	3.96*	3.93*	4.65*	4.06*	4.95*	6.43*	9.81*
MgO	1.06	0.88	0.95	0.90	1.28	0.96	1.52	2.31	3.70
CaO	3.09	2.36	2.45	2.44	3.02	2.57	3.19	5.15	6.62
Na_2O	4.39	4.69	4.34	4.15	3.39	4.15	4.49	3.48	3.08
K_2O	2.27	2.20	2.20	2.17	2.03	2.10	1.95	1.62	1.13
H_2O+	0.24	0.31	0.50	0.40	0.75	0.35	0.45	0.40	0.89
TiO_2	0.91	0.69	0.70	0.70	0.84	0.72	0.84	1.11	1.11
P_2O_5	0.18	0.17	0.34	0.23	0.45	0.31	0.36	0.11	0.35
MnO	0.11	0.11	0.11	0.11	0.12	0.15	0.13	0.16	0.18
Total	100.12	100.90	100.54	100.68	99.18	100.87	99.32	99.93	97.96

ERUPTIVE UNIT	Sveinagja ferrobasalts			Group I xenolith	Group II xenoliths		
	256	265	266	411	402	410	270
SiO_2	50.1	50.2	50.0	71.19	81.0	81.2	76.71
Al_2O_3	13.03	13.02	13.21	13.19	11.01	11.17	11.98
Fe_2O_3	3.39	3.36	3.82	2.53	0.73	-	1.48
FeO	12.68	12.69	12.61	2.29	1.98	2.69*	1.08
MgO	4.81	4.82	4.78	0.60	0.26	0.93	0.07
CaO	9.45	9.45	9.54	2.13	1.32	0.70	1.14
Na_2O	2.49	2.46	2.46	4.50	1.37	0.93	4.77
K_2O	0.52	0.52	0.53	2.28	2.15	2.00	2.32
H_2O+	0.13	0.31	0.14	0.40	0.50	0.41	0.51
TiO_2	2.83	2.82	2.78	0.59	0.20	0.38	0.17
P_2O_5	0.31	0.32	0.31	0.12	0.01	0.03	0.02
MnO	0.26	0.26	0.26	0.11	0.05	0.04	0.03
Total	100.00	100.23	100.44	99.93	100.58	100.48	100.28

FeO values with asterisks are total Fe as FeO.

Samples 256, 265, 266, 402, 410 analyzed by XRF and wet-chemical methods at the University of Lancaster; others by XRF and atomic absorption at the University of Rhode Island.

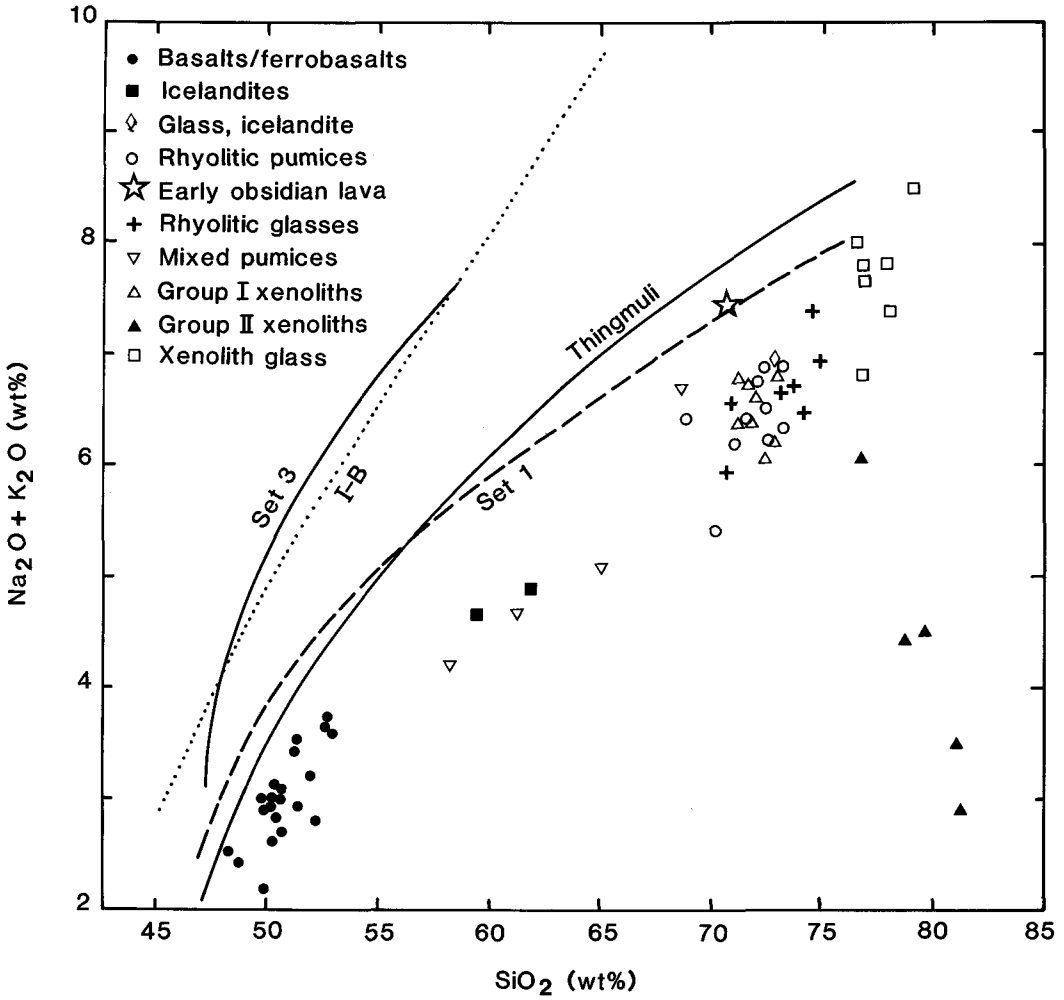

FIG. 1. Alkali–SiO_2 diagram, illustrating the tholeiitic affinity of Askja rocks. Data sources: this paper; Sigurdsson and Sparks (1981); Sigvaldason (1974); Wood *et al.* (1979). Trends for the Series 1 and 3 rocks of the Setberg volcanic centre from data in Sigurdsson (1970), for Thingmuli, Carmichael (1964). I–B dividing line between alkaline and subalkaline compositions from Irvine and Baragar (1971).

value of +9.7‰ was obtained for quartz standard NBS28. Sr and Nd isotope ratio precisions are better than ±0.00005 and 0.00001 respectively.

Geochemistry: general features

In common with other central volcanoes and associated fissure swarms in the northern active zone (Wood *et al.*, 1979), the Askja basalts and ferrobasalts are tholeiitic (Fig. 1), and follow a trend towards strong Fe- (and Ti-) enrichment (Fig. 2). The most mafic component of the 1875 eruption is a magnesian basalt (MgO = 7.73%) and there is a continuous compositional variation to evolved, ferrobasaltic rocks with MgO < 5%. The mafic components occur only as pumice clasts and glassy components of mixed rocks. It has not proved possible to separate sufficient quantities for conventional analysis, although electron microprobe data are available in Sigurdsson and Sparks (1981). Sigvaldason (1974) and Wood *et al.* (1979) have presented trace element data for glacial and post-glacial mafic lavas from Askja and we add three new analyses of Sveinagja ferrobasaltic lavas, erupted synchronously with the 1875 rhyolitic activity, some 70 km N. of Askja. Trace element

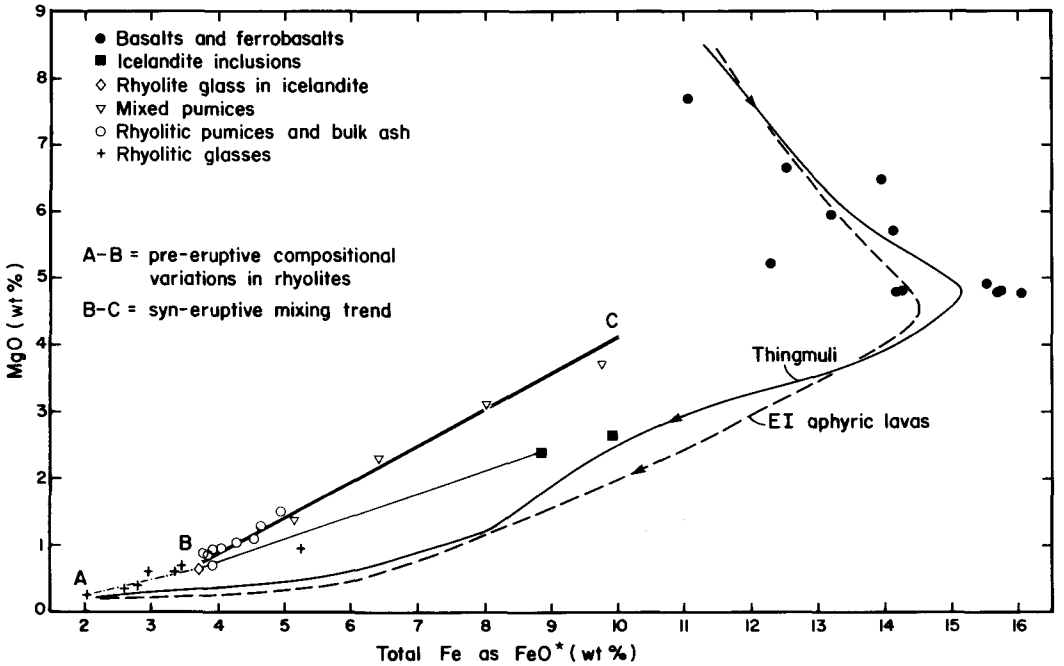

FIG. 2. MgO versus FeO_t for Askja rocks and comparative suites. Leucocratic xenoliths and glasses omitted for clarity. Askja data sources as for Fig. 1. Thingmuli trend—Carmichael (1964); that of east Iceland aphyric lavas—Wood (1978).

data, outlined below, confirm the suggestion of Sigurdsson and Sparks (1981) that these mafic lavas are broadly comparable to the mafic components of the 1875 eruption and can be used to approximate their compositions.

In more differentiated, non-mixed, rocks, there are two important compositional gaps, between ferrobasalt and icelandite and between icelandite and rhyolite (Figs. 1 and 2). The first of these gaps, together with the very small proportion (0.75%) of icelandite ejected in the 1875 eruption and the lack of icelandites in older Askja deposits, led Sigurdsson and Sparks (1981) to question the effectiveness of crystal fractionation in producing the more evolved members of the Askja suite. On the other hand, the major element features of the icelandites have been modelled by 50% crystallization of Sveinagja ferrobasalt using the phenocryst assemblage 1.8 plagioclase: 2.3 augite: 1 magnetite (Sigurdsson and Sparks, 1981), and the inferred liquid line of descent (Fig. 2) is similar to those of the Thingmuli and eastern Iceland suites, where intermediate rocks form a larger proportion of the eruptive sequences. We consider the icelandites to be an integral part of the differentiation sequence basalt–rhyolite at Askja.

The differentiation trend from icelandite to rhyolite is represented by the icelandite rock–glass tie-line in Fig. 2. It has been drawn arbitrarily straight but almost certainly followed a curved path in nature, similar to that of the Thingmuli suite. The analysis of an iron-rich rhyolitic shard in a welded tuff (Sigurdsson and Sparks, 1981, Table 8, no. 3) would lie on such a curve and partially fills the compositional gap between icelandite and rhyolite. We suggest that a more complete sequence of liquids between these two was available in the magma chamber than was erupted in 1875 and/or analysed by us. The composition of the glass in the icelandite inclusion lies very close to that of the least magnesian, bulk rhyolitic pumice (As 100). Certain aspects of the trace element chemistry of this rock, e.g. high Rb and Rb/Sr and low Sc (Table 1), suggest that As 100 approximates the least differentiated rhyolite *liquid* so far sampled in the system; more 'mafic' rhyolites are clearly mixtures of basalt and rhyolite (Fig. 2).

Three further types of rhyolitic liquids can be distinguished (Figs. 2, 3); rhyolite glasses in pumices; mixtures of basalt and rhyolite in mixed pumices producing composite liquids of incompletely mixed or stirred basalt and rhyolite liquids; and rhyolitic pumices representing more thorough mixing of basalt and rhyolite.

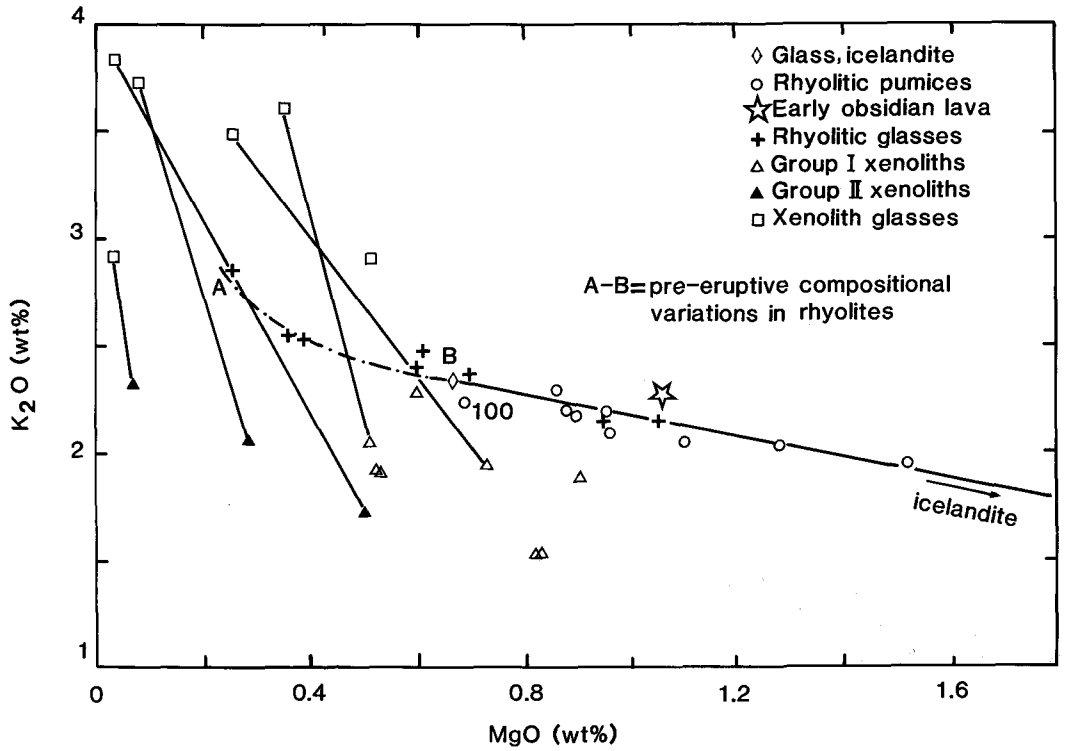

FIG. 3. MgO–K_2O plot for low-MgO Askja rocks. A tie-line connects icelandite inclusion (off plot) and glass. Tie-lines also connect leucocratic xenoliths and coexisting glass. Mixed pumices omitted; the mixing line is close to the icelandite rock–glass tie-line.

The first, the rhyolite glasses of Sigurdsson and Sparks (1981), occur only as a glassy component of mixed pumices, lavas and welded tuffs. They lie on the low-Mg extension of the icelandite rock–glass tie-line, in a position qualitatively consistent with their being the fractionation product of As 100-type silicic magma (trend B in Fig. 2 and line A–B in Fig. 3). We interpret these glasses as representing the compositional variation *within* the pre-eruption rhyolitic cap of the Askja magma chamber.

The second type of rhyolitic liquids is represented by the rocks referred to as mixed pumices, which are composed of megascopic mixtures of brown rhyolitic and Mg-rich basaltic glasses, formed by incomplete stirring of two liquids. A third type comprises rhyolitic pumices (other than As 100, see above) and bulk tephra, which appear to represent more thorough mixing of basaltic and rhyolitic liquids on a finer scale than the mixed pumices. An MgO–FeO_t plot (Fig. 2) shows that the majority of analysed pumices lie on the same mixing line as the mixed pumices, with admixture of up to 10% basalt. The diagram also neatly stresses the point, appreciated by Sigurdsson and Sparks (1981), that the mafic component of these mixed rocks is not Sveinagja ferrobasalt, but more magnesian basalt, comparable with lavas erupted prior to 1875 at Askja. Extrapolation of line BC indicates an MgO concentration of c. 6% for this component; comparable results are obtained using, for example, MgO–TiO_2 and MgO–Eu plots.

Microprobe analyses of glasses (Sigurdsson and Sparks, 1981) indicate that silicic liquids formed by partial melting of the leucocratic xenoliths are more potassic than the rhyolitic glasses and pumices and their host xenoliths (Fig. 3). These glasses associated with the xenoliths cannot be separated for trace element analysis but, on the basis of major element relationships (e.g. Fig. 3), a component of partial fusion liquids in the rhyolite glasses cannot be precluded. Judging from the potassic nature of the xenolith glasses, it might be predicted that the liquids were also high in Rb, Th, U and Cs.

On the basis of major element compositions, Sigurdsson and Sparks (1981) recognised two distinct groups among the leucocratic xenoliths.

Group 1 xenoliths show an overall similarity to the rhyolitic pumices, although they are slightly lower in CaO, TiO_2 and K_2O and higher in Na_2O and FeO_t, at similar levels of MgO. Small trace element differences, notably higher Zr and Hf and lower Rb, also exist. We interpret these xenoliths as representing silicic magmas, earlier than and composition similar to, those of the rhyolitic pumices, but with sufficient minor differences to indicate a somewhat different lineage.

On the basis of the trace element data, xenolith As 413 appears to have an intermediate composition, similar to that of the icelandite inclusions. This suggests that the xenoliths may be part of a wider suite of magmatic compositions from an earlier phase of activity, and that icelandite magma was possibly more abundant in the magma chamber than among the erupted products.

The xenoliths of Group II are SiO_2-rich (76–81%) and poor in femic components and Al_2O_3. Sigurdsson and Sparks (1981) questioned whether they represented magmatic compositions, while Sigvaldason (1979) noted that these rocks had been hydrothermally altered. The evidence is persuasive:

(i) The compositional variability, especially in Na_2O, Na_2O/K_2O, MgO, Sr and Pb.
(ii) The presence of quartz veins in some samples.
(iii) The very low δO^{18} values (+1.0 to −9.9‰, Muehlenbachs *et al.*, 1974; Sigvaldason, 1979; this paper, Table 4) indicating interaction with meteoric water.
(iv) SiO_2 values higher than those in any pristine rhyolitic obsidian (Macdonald *et al.*, in prep.).

Compositional variation related to hydrothermal processes makes the chemistry of Group II more difficult to interpret. Trace element data make it clear, however, that they represent a different lineage to both the rhyolite pumices and the Group I xenoliths. Despite the diluting aspect of SiO_2 addition, the Group II rocks have lower contents of TiO_2 and Sc, and higher Nb, Ta, Y and the *REE*, especially *HREE*. The ratios of Ta/Zr and Ce/Zr also differ, and they have the strongest negative Eu anomalies in the suite.

Petrogenesis

The petrogenetic model of the 1875 eruption presented by Sigurdsson and Sparks (1981) is now assessed in the light of selected trace element and isotopic data. We concentrate on two topics. On the origin of the magnesian basalt–icelandite sequence there is a broad agreement (Wood *et al.*, 1979; Sigurdsson and Sparks, 1981) that crystal fractionation was the dominant mechanism. A more debatable topic is the origin of the rhyolites. Wood *et al.* (1979) considered them to have formed by extreme fractional crystallisation of the basalts (cf. Carmichael, 1964; Wood, 1978). While unable to preclude this mechanism, Sigurdsson and Sparks (1981) preferred a more complex explanation. They envisaged total melting of the silicic xenoliths and mixing with 7–14% of Sveinagja ferrobasalt to produce dacitic hybrids comparable in composition to specimens As 103 and As 229. 10–11% fractional crystallisation of a plagioclase-

Table 3. Modelling parameters in Rayleigh fractionation

Interval	Phenocryst assemblage	Mass fraction	PARTITION COEFFICIENTS									
			Ba	Hf	Rb	Sr	Ta	Th	La	Ce	Tb	Yb
Basalt + ferrobasalt	Plagioclase	0.56	0.20	0.01	0.07	–	0.01	–	–	–	–	–
	Augite	0.37	0.00	0.10	0.02	–	0.10	–	–	–	–	–
	Fe-Ti-oxides	0.07	0.00	0.28	0.00*	–	2.0	–	–	–	–	–
	Apatite	0.001	0.00	0.00*	0.00	–	0.00*	–	–	–	–	–
Ferrobasalt + icelandite	Plagioclase	0.35	–	0.02	0.10	–	0.01	–	0.11	0.12	0.05	0.067
	Augite	0.45	–	0.50	0.02	–	0.15	–	0.15	0.15	1.00	0.62
	Fe-Ti-oxides	0.196	–	0.90	0.00*	–	2.0	–	0.29	0.29	0.50	0.50
	Apatite	0.0034	–	0.00*	0.00	–	0.00*	–	10.0	10.0	20.0	10.0
Icelandite + rhyolite	Plagioclase	0.53	–	0.03	–	2.7	0.01	0.10	0.20	0.18	0.07	0.070
	Augite	0.30	–	0.80	–	0.12	0.20	0.00	0.20	0.18	0.80	1.20
	Fe-Ti-oxides	0.15	–	2.00	–	0.00*	4.0	0.00*	0.30	0.30	0.50	1.00
	Apatite	0.017	–	0.00*	–	3.0	0.00	0.50	20.0	20.0	40.0	15.0

Partition coefficients selected from ranges given in Arth (1976), Sun and Hanson (1976), Irving (1978), Schock (1979) and Henderson (1982).

Values with asterisks have been arbitrarily set at zero. $K_{Th}^{apatite/liq.}$ also arbitrary.

clinopyroxene–Fe–Ti-oxides assemblage from the dacitic liquids produced the (pre-mixing) compositional variations in the rhyolites.

The approach adopted here is to test trace element distributions for consistency with the fractional crystallization scheme outlined above on the basis of MgO–FeO_t relationships. Much use is made of modelled Rayleigh fractionation trends. The various parameters used are given in Table 3.

Table 4. O, Sr and Nd isotopic data for Askja rocks

	$\delta^{18}O$ ‰ (SMOW)	$^{87}Sr/^{86}Sr$	$^{143}Nd/^{144}Nd$
Rhyolitic pumice			
As 108	+2.5	0.70318	-
As 102	+0.8	0.70313	-
Mixed pumice			
As 229	+0.7	0.70317	0.51300
Ferrobasalt			
As 256	+5.5	0.70315	0.51304
Group I xenoliths			
As 275	+2.8	-	-
As 412A	-9.0	0.70317	-
Group II xenoliths			
As 402	-6.7	-	-
As 270	-8.3	0.70316	-

Constant phenocryst assemblages within each crystallisation interval are assumed. We appreciate that the results of such models are highly dependent on the solid/liquid partition coefficients employed, which are normally selected from the wide range available in the literature. They are, therefore, to some degree subjective, at best *consistent* with the given genetic model. We shall show, however, cases where the Askja data are not consistent with simple, closed-system, crystal fractionation, thus demanding a more complex origin.

Rare earth elements

REE distribution is summarized on MgO diagrams (Fig. 4) and on chondrite-normalised plots (Fig. 5). The *LREE* show different behaviour to the intermediate and *HREE*, in that the *LREE* abundances increase steadily from basalts to icelandites to rhyolites, while the intermediate- and *HREE* have similar abundances in icelandites and rhyolites. Thus ratios of light : intermediate and light : heavy *REE* increase with progressive fractionation (Figs. 5, 6).

The increase in Ce/Yb ratio apparently contrasts with the situation at other Icelandic centres. Wood *et al.* (1979) suggest that even during the 90% crystal fractionation required to produce silicic residual liquids from magnesian basaltic parents, the Ce/Yb ratio increases by only a factor of 0.2. We have explored this apparently anomalous behaviour using trace element modelling. Lack of *HREE* data for the magnesian basalts means that only the ferrobasalt–rhyolite sequence can be considered.

First, it is important to constrain the amount of apatite in the fractionating assemblage, since apatite is very efficient in changing the ratio of intermediate *REE* to *LREE* and *HREE* in residual liquids (Wood, 1978). Mass balance calculations using values of 0.32, 0.50 and 0.30% P_2O_5 in the ferrobasalts, icelandites and rhyolites respectively, and 42% P_2O_5 in apatite (Wood, 1978, Table 9) indicate that the maximum mass fraction in the interval ferrobasalt–icelandite was 0·0017 and in the interval icelandite–rhyolite 0.0083.

The model provides a very good fit between the icelandites and the residual liquids formed by $\sim$ 50% fractional crystallisation of the ferrobasalts (c.f. Sigurdsson and Sparks, 1981, p. 65).

It is also possible to derive the *REE* characteristics of the rhyolites by crystal fractionation, in this case the composition of As 100 representing some 75% crystallisation of the parental ferrobasalt or 50% crystallisation of the icelandite. The model requires an increased partitioning of *HREE* into clinopyroxene $\pm$ oxides but the $K_{Yb}^{cpx/liq}$ and $K_{Yb}^{ox/liq}$ values of 1.20 and 1.00 are not unreasonable (Arth, 1976; Irving, 1978; Schock, 1979).

The sequence magnesian basalt–rhyolite is marked at Askja by the development of significant, negative Eu anomalies in the rhyolites (Fig. 5). By using the parameters in Table 3, it is possible to model Eu behaviour as follows: basalt–ferrobasalt, $D = 0.65$, $f = 0.3$; ferrobasalt–icelandite, $D = 0.80$, $f = 0.15$; icelandite–rhyolite, $D = 1.30$, $f = 0.08$. Considering the strong partitioning of Eu into plagioclase, the D values are reasonable, and the f values are in line with the modelling for other trace elements reported here.

Thus, although such models are no better than the arbitrary choice of partition coefficients, there is no strong evidence from the *REE* that a process other than fractional crystallisation is required to derive the rhyolites from the ferrobasalts.

Rb–Hf plot

This plot (Fig. 7) is useful in that the different Rb/Hf ratios in the rhyolites and the xenoliths

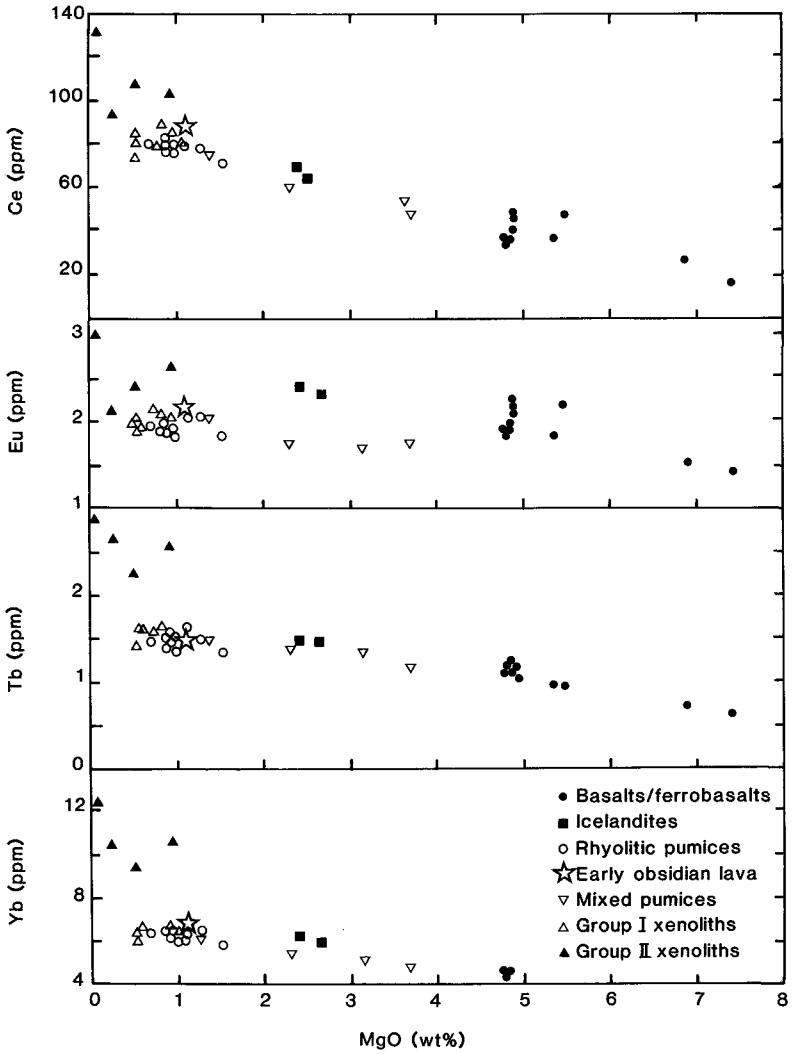

FIG. 4. MgO–*REE* plots. Data sources as in Fig. 1. Note the overall similarity of the rhyolitic pumices and Group I xenoliths, and the *REE*-enriched nature of the Group II xenoliths.

permit the Sigurdsson and Sparks (1981) mechanism for the origin of the rhyolitic magmas to be tested. The zone of potential melts formed by total fusion of Group I xenoliths followed by 7–14% mixing with Sveinagja ferrobasalt is shown. It does not encompass specimens As 103 or As 229, selected as rocks likely to have formed by this two-stage mechanism (Sigurdsson and Sparks, 1981).

An alternative explanation is that *partial fusion* of Group I xenoliths produced liquids which had relatively high Rb/Hf ratios (say 7–8), which then mixed with basaltic magmas. The potassic nature of the xenolithic glasses (Fig. 3) would be consistent with such a model. We cannot preclude this mechanism on chemical grounds but question its efficiency because of physical difficulties. The intimate, interpenetrating textures seen in the partially molten xenoliths, including fingerprint and sieve textures, suggest to us that it is unlikely that partial melt and residue could separate efficiently.

The quasi-linear correlation betwen Rb and Hf would seem, on the other hand, consistent with fractional crystallisation and we have attempted to model the variation using Rayleigh fractionation. The interval magnesian basalt–ferrobasalt is satisfactorily modelled, using low bulk distribution

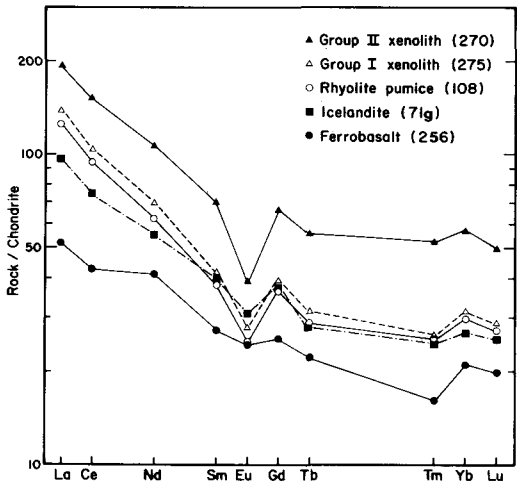

FIG. 5. Chondrite-normalised *REE* plots. Normalising factors from Nakamura (1974), except Tb and Tm, from Thompson (1982).

coefficients for both Rb and Hf (Table 3). The ferrobasalts represent between 60% and 70% crystallisation of the assumed parental basalt.

The model is much less successful in more evolved compositions. The range of Hf concentrations is reached after about 75% crystallisation of the ferrobasalt, some 90% of the original basalt. Even at such low f values, it is notable that the Rb values predicted by the model are only half those in the most evolved rhyolites. To achieve a better fit, the bulk distribution coefficient for Hf would have to be increased significantly over the 0.40 used in the model. This is not unrealistic. The $K_{Hf}^{cpx/liq}$ and $K_{Hf}^{ox/liq}$ values of 0.50 and 0.90 employed are similar to those for mafic rocks reported by Schock (1979) and Henderson (1982), but a higher bulk distribution coefficient would mean that Hf could hardly be considered an incompatible element in the Askja suite.

The Rb–Hf modelling reveals a critically important point in the Askja data: the six- to sevenfold increase in Rb concentrations between ferrobasalts and rhyolites is exceedingly difficult to reconcile either with major element modelling (Wood, 1978; Sigurdsson and Sparks, 1981) or with the behaviour of the High Field Strength (HFS) elements, such as Hf, Zr, Nb and Ta. Our interpretation is that Rb has been added to the Askja rhyolites by a process other than, but complementary to, fractional crystallisation.

Rb–Ba plot

The only phenocryst phase into which Rb and Ba partition significantly during fractionation of tholeiitic basalt is plagioclase. The average $K_{Ba}^{plag/liq}$

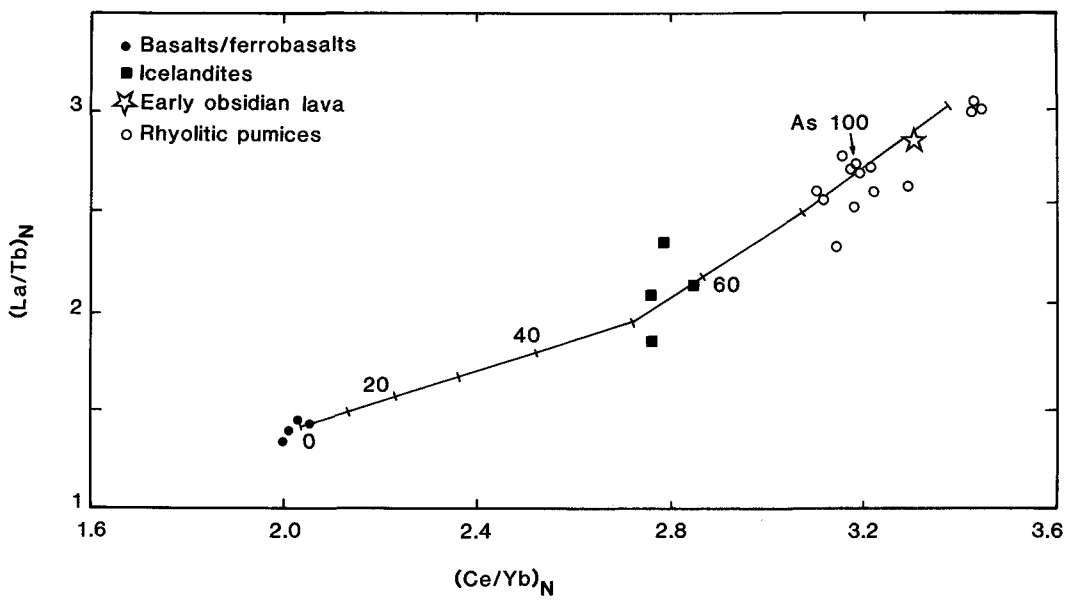

FIG. 6. $(Ce/Yb)_N$ versus $(La/Tb)_N$ plot for Askja rocks. Labelled line indicates Rayleigh fractionation path and percent crystallised for a ferrobasalt parent magma, using parameters in Table 3.

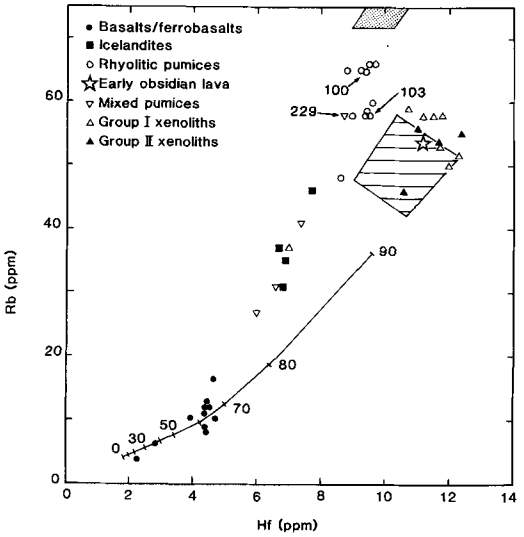

FIG. 7. Rb versus Hf plot for Askja rocks. Ruled field indicates potential melts formed by total fusion of Group I xenoliths followed by mixing with 7–14% of Sveinagja ferrobasalt. Dotted area is hypothetical field of liquids formed by partial fusion of xenoliths. Labelled line indicates Rayleigh fractionation path and percent crystallized for a basaltic parent magma (Rb = 4 ppm, Hf = 1.8 ppm), using parameters in Table 3.

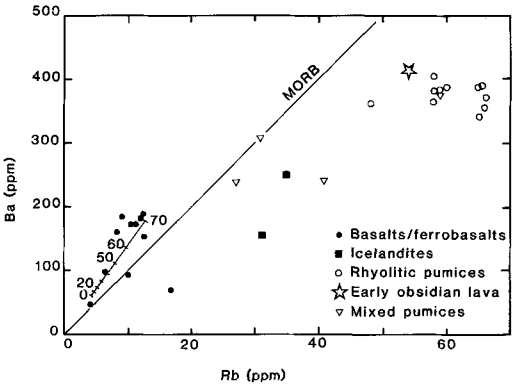

FIG. 8. Rb–Ba plot. Labelled line is Rayleigh fractionation path and percent crystallised for parental basaltic magma (Rb = 4 ppm, Ba = 60 ppm). MORB ratio of 10 from Pearce (1982).

and $K_{Rb}^{plag/liq}$ for basalt and andesitic rocks are 0.23 and 0.07 respectively (Arth, 1976), indicating that the Ba/Rb ratio will progressively decrease through fractionation. This is the type of behaviour shown in the Askja suite (Fig. 8), the basalts and ferrobasalts having a Ba/Rb ratio slightly above that in average MORB, while the silicic rocks show relative Rb-enrichment. We have attempted to model this distribution using the parameters in Table 3 and a parental basalt with Rb = 4 ppm and Ba = 60 ppm.

There is a satisfactory fit between the parental basalt and the ferrobasalts, the amount of crystallisation being 70%, which is comparable to the 70% calculated from the Eu data, and to the 66% calculated, on the basis of major element modelling, for the Tertiary lavas of eastern Iceland by Wood (1978).

The sequence ferrobasalt → rhyolite is more difficult to model by fractional crystallisation. Rb increases five-fold, from 12 to 60 ppm, which, assuming $K_{Rb}^{plag/liq}$ to be $\leqslant 0.1$, indicates an f-value of about 0.2. Over the same interval, Ba concentrations approximately double. Even assuming the plagioclase fraction of the crystallising assemblage to be 0.6, these figures infer $K_{Ba}^{plag/liq} \geqslant 1$, which is considerably higher than any value compiled by Arth (1976) or Henderson (1982). An alternative explanation would seem to be that even though fractional crystallisation was operative, another process enriched the residual liquids in Rb relative to Ba, confirming the conclusion based on Rb–Hf relationships.

We suggest that critical evidence as to the nature of the Rb-enriching process comes from the Cs data. The basalt–ferrobasalt–icelandite sequence shows an essentially linear relationship between Rb and Cs (Fig. 9), the trend extrapolating through the origin, as would be expected from essentially incompatible behaviour in mafic melts. Two of the rhyolites follow this trend, but most have a signi-

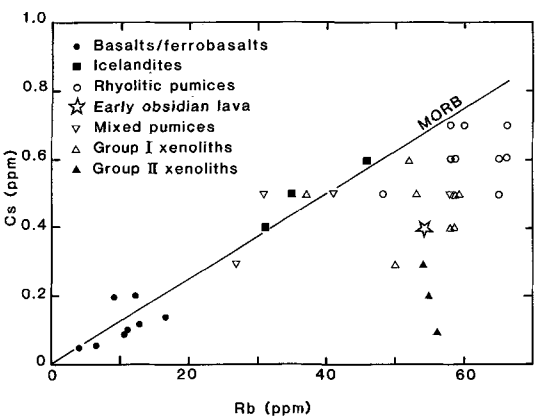

FIG. 9. Rb versus Cs plot. Rb/Cs ratios of rhyolitic pumices are higher than those of more mafic rocks, but comparable to those in the leucocratic xenoliths. MORB ratio shown for reference.

ficantly lower Cs/Rb ratio. It is not possible that Cs could be incorporated preferentially to Rb into a plagioclase-augite-oxide-apatite fractionating assemblage. We suggest an alternative explanation: the low Cs of the rhyolites is related to a component derived from the leucocratic xenoliths, which had earlier been depleted in Cs during hydrothermal alteration.

Sr/Ta-Th/Ta plot

Over the interval magnesian basalt to ferrobasalt, Th and Ta both had very low bulk distribution coefficients, such that the Th/Ta ratio was nearly constant (Fig. 10). Removal of Sr by plagioclase fractionation led to a rapid decrease in Sr/Ta ratio. Fe-Ti oxides joined the fractionating assemblage at the ferrobasalt stage and presumed partitioning of Ta into this phase resulted in a less rapid decrease in Sr/Ta ratio, and rise in Th/Ta ratio, as the residual liquids moved towards icelandite. This combination of elements (of different compatibilities) might be expected to provide clues as to genetic mechanisms.

Fig. 10 shows two attempts to model the fractional crystallisation of icelandite to rhyolite. Model 1 employs the calculated *bulk* distribution coefficients for Sr and Ta used by Wood (1978, p. 426) to model the same compositional interval in Tertiary lavas of eastern Iceland. The partition coefficient for Th was here selected arbitrarily, but must be low (Benjamin *et al.*, 1978, 1980; Clague and Frey, 1982). Model 1 fails to match the Askja data, because the low partition coefficients chosen for Th and Ta make it difficult to reproduce the increase in Th/Ta ratio in the Askja rhyolites.

Model 2, which provides a better fit, was achieved by assuming a *relatively* (but not abnormally) low $K_{Sr}^{plag/liq}$ value and a high $K_{Ta}^{ox/liq}$ of 4.

Using the model, As 100 would have been formed by 40–45% crystallisation of the icelandite parent, which is comparable to the 50% crystallisation calculated from major element data by Sigurdsson and Sparks (1981). The success of model 2 depends largely on whether the $K_{Ta}^{ox/liq}$ value of 4 is acceptable, bearing in mind that the Fe-Ti oxides are almost certainly the main carrier of Ta in tholeiitic suites (Gottfried *et al.*, 1968). We note that Schock (1979) records empirical Ta partition coefficients of 1–10 for magnetites crystallised from ocean-floor basalts. The bulk distribution coefficient for Ta used in the calculations is certainly consistent with Hf-Ta relationships, which show a marked increase in Hf/Ta ratio in the rhyolites (Fig. 11). We infer,

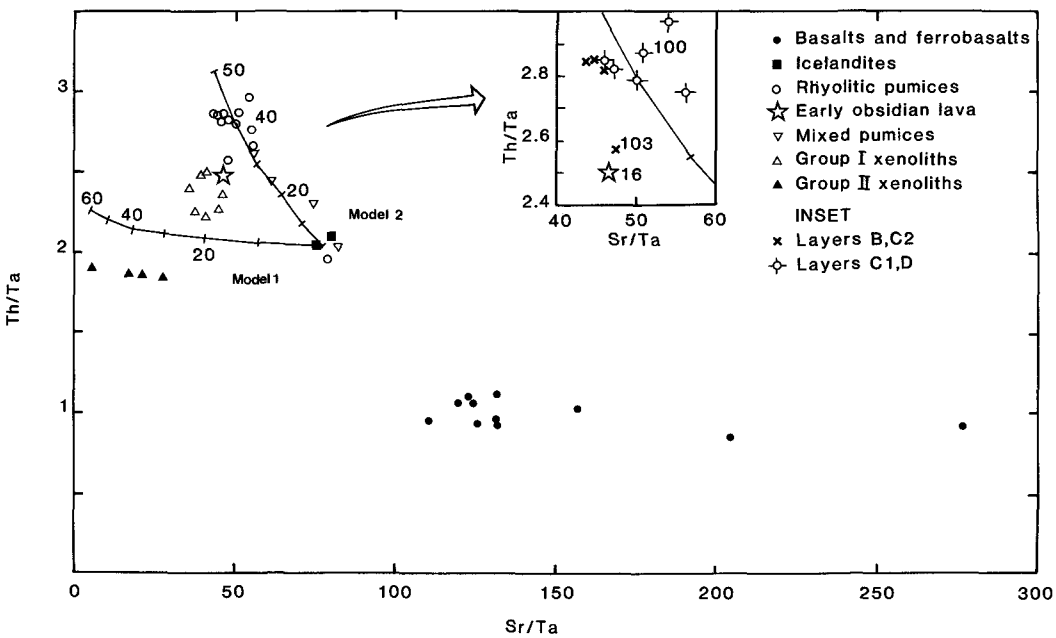

FIG. 10. Sr/Ta-Th/Ta plot for Askja rocks. Two Rayleigh fractionation models are presented. Model 1 uses bulk distribution coefficients from Wood's (1978) study of eastern Iceland basalts. Model 2 uses parameters in Table 3: figures on path refer to percent crystallised of ferrobasalt parent. The enclosed inset shows the data points for the rhyolitic pumices and early obsidian flow in greater detail, with symbols representing stratigraphic position.

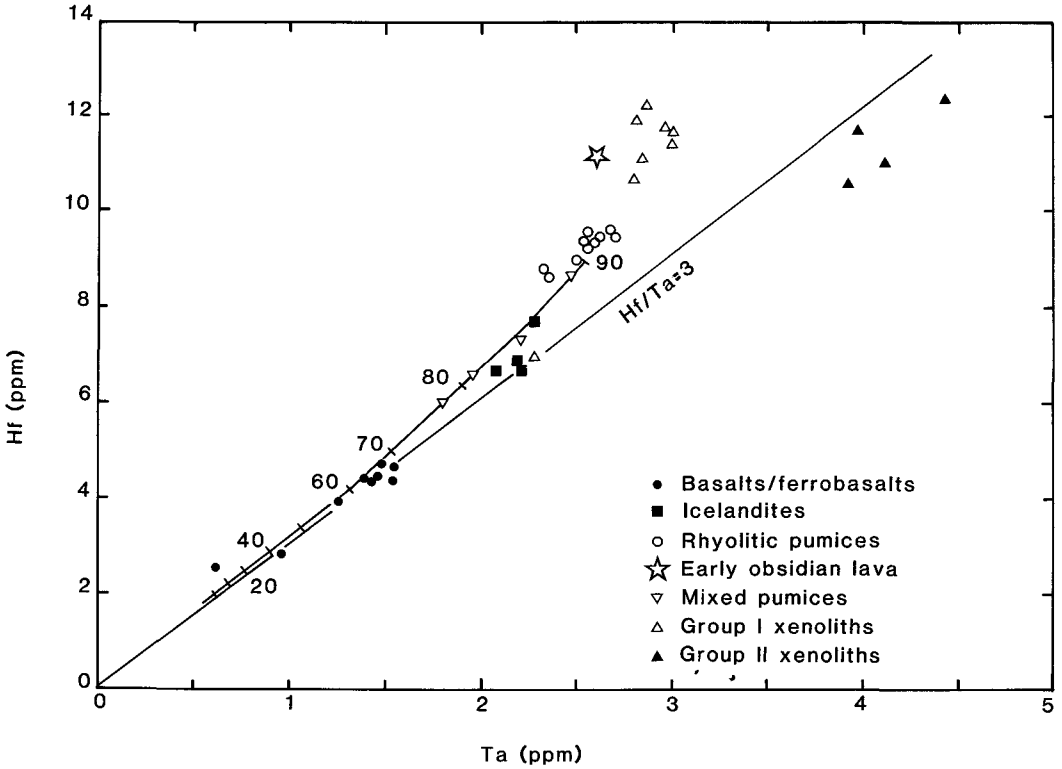

FIG. 11. Ta versus Hf plot. Note the similar bulk distribution coefficients inferred for the basalt–icelandite sequence, but the increased partitioning of Ta into the solids in the interval icelandite–rhyolite. Note also the different Ta/Hf ratios of the Group II xenoliths.

therefore, that the icelandite–rhyolite sequence at Askja was generated largely by fractional crystallisation.

There is, nevertheless, some evidence on the Sr/Ta–Th/Ta plot (Fig. 10) of a more complex situation. Specimens As 103 (rhyolite pumice of C2 layer) and As 16 (early obsidian flow) plot with the Group I xenoliths rather than the other rhyolitic eruptives. It may also be noted that As 16 has higher Zr, Hf and *LREE* contents than the other rhyolites. These features suggest a 'xenolithic' component in the trace element composition of these rocks, and draw attention to a possible cross-trend in the trace element data (Fig. 10). In detail (inset, Fig. 10), the products of the later phases of the pyroclastic activity (C1 and D layers) fall to the right of, or on, the modelled trend, while rocks of earlier phases (As 16, 103) are displaced towards the xenolith field. While accepting the very tenuous nature of the evidence, we suggest the following interpretation. Fractional crystallisation of icelandite magmas produced silicic residua comparable to As 100. A discrete set of silicic liquids was also produced by partial melting of the source rocks of the Group I xenoliths. Though the trace element chemistry of these melts is unknown, it can be reasonably inferred that they had higher Th/Ta and lower Sr/Ta ratios than the parent granitic rocks. The pumices which fall on the cross-trend were formed by mixing of the two types of rhyolite. As 103 and As 16 must represent a high proportion of xenolith derived partial melt in terms of these trace elements.

Isotopic data

O, Sr and Nd data are listed in Table 4. $^{87}Sr/^{86}Sr$ ratios vary from 0.70313 to 0.70318 (6 analyses), while $^{143}Nd/^{144}Nd$ varies from 0.51300 to 0.51304 (2 analyses). The limited variation in the radiogenic isotope ratios over the compositional spectrum is a characteristic feature of Icelandic rift zone volcanic centres (Wood *et al.*, 1979; Condomines *et al*, 1983; Oskarsson *et al.*, 1982; 1985). According to

Oskarsson *et al.* (1985), who adopted the three-source model of Zindler *et al.* (1982, 1984), there are three radiogenic isotope reservoirs involved in the formation of the Icelandic rock suites: (1) the single mantle source; (2) reworked oceanic plate composed of basalts; and (3) silicic volcanic centres embedded in the old plate. The most radiogenic Icelandic rocks (high $^{87}Sr/^{86}Sr$) are silicic rocks from long-lived volcanic centres which continued to evolve even after they migrated away from the central rifts, and thus they contain the largest component of reworked crust. Rocks erupted from central regions of the Iceland rift have the low $^{87}Sr/^{86}Sr$ ratios and high $^{143}Nd/^{144}Nd$ ratios characteristic of magmas with a reservoir (1) isotopic signature. The Sr and Nd isotopic ratios of Askja magmas, which lie largely within the 'volcanic centre' array of Oskarsson *et al.* (1985), suggest that their Sr and Nd isotopic signatures are derived from reservoir (1), the single mantle source. From this it may be assumed that the initial oxygen isotopic value of Askja rocks will be around +5.5 to +5.6‰, the Icelandic mantle value (Muehlenbachs, 1973; Muehlenbachs *et al.*, 1974; Oskarsson *et al.*, 1982). Any deviations from this at Askja should therefore be attributed to processes occurring at high crustal levels in the sub-volcanic environment and not reflect source region $\delta^{18}O$ heterogeneities.

The Askja oxygen isotope data are listed in Table 4. Using these and data from Muehlenbachs (1973), Muehlenbachs *et al.* (1974), Hattori and Muehlenbachs (1982) and Condomines *et al.* (1983), Fig. 12 has been constructed showing the $\delta^{18}O$ ranges of Askja rocks, compared with the $\delta^{18}O$ ranges in Icelandic rhyolites, basalts, the Hekla volcano, and drill hole data. For the Askja data, a continuum exists from 'normal' mantle $\delta^{18}O$ in the Sveinagja basalt (+5.5 ‰) to slightly ^{18}O-depleted basalts within Askja (+3.6 to +3.0‰), through to ^{18}O-depleted rhyolites (+2.5 to +0.4‰). While the xenoliths range from +2.8 to −9.9‰, over 90% lie within the range −4.7 to −9.9‰. The Group II xenoliths are the most ^{18}O depleted (−4.7 to −9.9‰). The less altered Group I xenoliths are more variable, with $\delta^{18}O$ values ranging from +2.8 to −9.0.

Comparing the Askja data with the rest of Iceland, the Askja basalts are by no means unique in their ^{18}O-depleted nature (+3.0 to +3.6‰), though the Icelandic mode lies aroung +4.4‰. The Askja rhyolites, however, are depleted in ^{18}O by around 3‰ relative to other Icelandic silicic rocks, 2‰ greater than the Askja basalt ^{18}O depletion. In Fig. 12 the $\delta^{18}O$ values for the IRDP core (39.20 m to 1909.89 m), for the RD-34 Reykjavik drillhole (31 m to 3085 m), and for the KG 4-12 drillholes at Krafla are also presented (data from Hattori and Muehlenbachs, 1982). The IRDP core and the Reykjavik drill hole show slight ^{18}O depletion relative to Iceland basalts, this being most pronounced in the latter. The most striking ^{18}O depleted values are found in the Krafla drill holes, with $\delta^{18}O$ values ranging from −3.4 to −10.5‰. This range encompasses the entire range of the Askja xenolith suite (with the sole exception of anomalous xenolith As-275), and provides strong evidence for the hydrothermal alteration and oxygen isotopic exchange of the Askja xenoliths.

The source of ^{18}O depletion has previously been constrained to the upper crust as Sr and Nd isotopic ratios provide no evidence for reworking of old (and presumably ^{18}O depleted—Oskarsson *et al.*, 1982, 1985) crustal materials. The obvious reservoir of isotopically light ^{18}O is meteoric water, which Sigvaldason (1979) calculated to have a value of −12.93‰ in the Askja region. Note that $\delta^{18}O$ values of −55‰ have been reported from polar regions (Epstein *et al.*, 1970). Studies by Taylor and Forester (1971) on the Tertiary Hebridean igneous complexes of western Scotland showed that circulation of comparably ^{18}O-depleted (−12‰) meteoric water in a hydrothermal system resulted in maximum ^{18}O depletion in the core regions of the complexes, where interaction temperatures were highest and water-rock ratios most elevated (see also Sheppard, 1977). 'Normal' values were found in rocks erupted at a significant distance from the central complexes, i.e. outwith the hydrothermal flow net. It is important to note that of the 200 $\delta^{18}O$ determinations of Icelandic rocks, no comprehensive study of one volcanic centre comparable with the detailed studies of Taylor and Forester (1971) has been carried out. Thus we have adopted their model for the interpretation of $\delta^{18}O$ variations observed in the Askja rocks. The most ^{18}O-depleted rocks (the leucocratic xenoliths) are inferred to have predated the 1875 rhyolite magmas and thus to have experienced the greatest amount of hydrothermal alteration with attendant isotopic exchange with ^{18}O-depleted meteoric waters. Askja basalt magmas, inferred to underlie rhyolite magmas in magma chamber reconstructions (Sigurdsson and Sparks, 1981), would experience the lowest degrees of hydrothermal alteration and isotopic exchange, primarily as a result of their depth of residence being outside the major flow lines of the circulation system. On this point it is interesting to note that the $\delta^{18}O$ of Askja basalts erupted within the main caldera is +3.0 to 3.6‰, while the $\delta^{18}O$ of a Sveinagja ferrobasalt erupted to 70 km distant is +5.5‰. This provides some evidence for the ^{18}O depletion of erupted magmas being constrained to within the central volcanic edifice and at upper crustal levels.

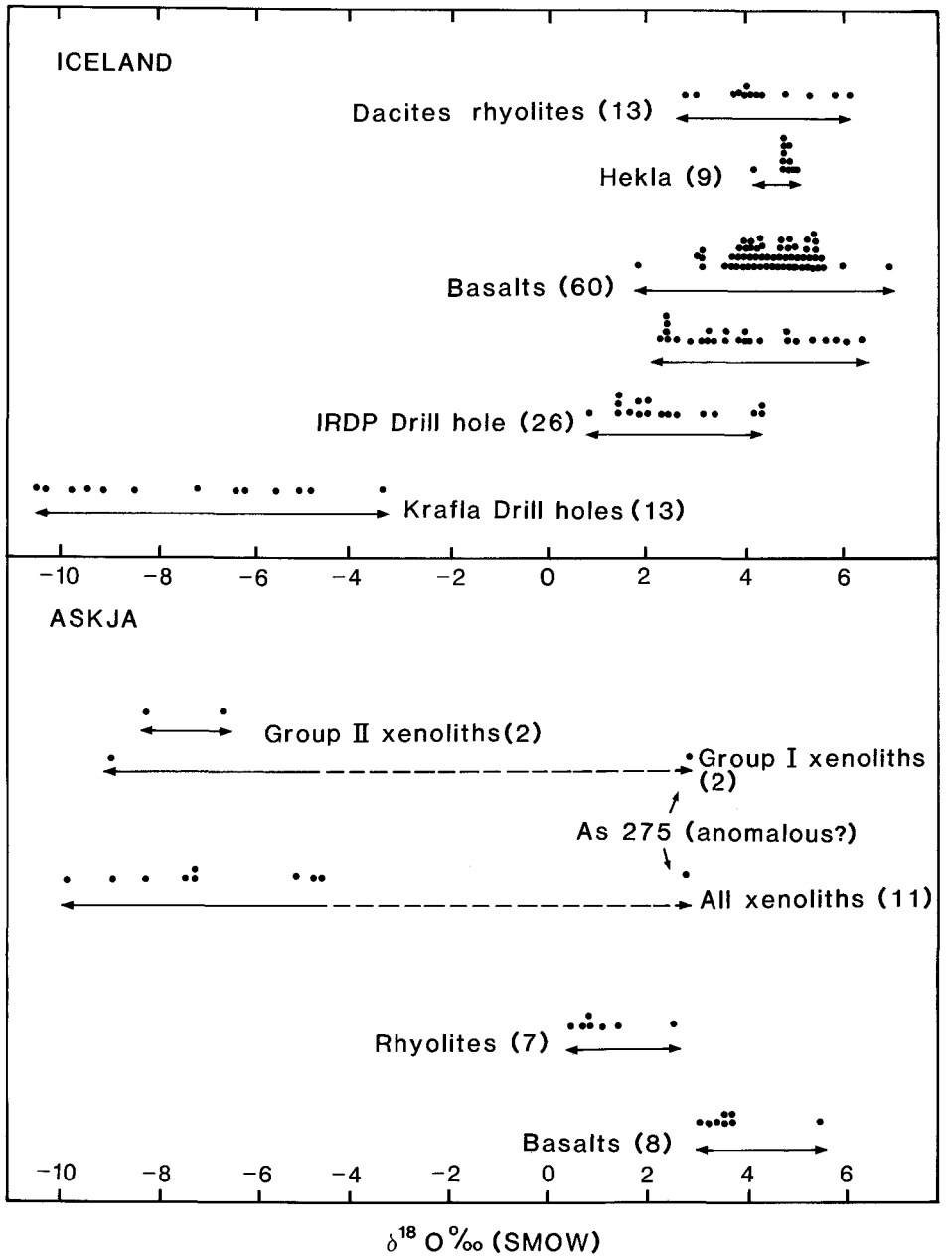

FIG. 12. (*a*) Ranges of $\delta^{18}O$ values (individually given as dots) in Icelandic basalts and rhyolites, the Hekla volcano, and various drill holes, compiled from data in Muehlenbachs (1973). Muehlenbachs *et al.* (1974), Hattori and Muehlenbachs (1982) and Condomines *et al.* (1983). Numbers of samples given in brackets. (*b*) Similar data for the Askja rocks, from Muehlenbachs (1973), Muehlenbachs *et al.* (1974), Condomines *et al.* (1983) and this paper, Table 4.

The ^{18}O-depleted nature of the rhyolites could be the result of four processes: (*a*) fractional crystallisation of basalt produced rhyolitic liquids depleted in ^{18}O due to isotopic fractionation between liquids and crystallising phases; (*b*) isotopic fractionation during superheating of the rhyolite magma during injection of hot basalt into the chamber (cf. Sparks *et al.*, 1977); (*c*) rhyolite magma, previously formed by fractionation of basalt and having a 'normal' isotopic signature (around +5.5‰), isotopically exchanged with ^{18}O depleted meteoric waters during residence in the chamber; (*d*) rhyolite magmas became ^{18}O depleted due to isotopic exchange with extremely ^{18}O depleted wall rocks, either via assimilation of wall rock material or during selective isotopic exchange.

As regards mechanism (*a*), although variations in $\delta^{18}O$ of up to 2.0‰ have been recorded during basalt to rhyolite fractionation (Taylor and Epstein, 1962; Taylor, 1968; Garlick *et al.*, 1971; Muehlenbachs and Byerly, 1982), fractionation resulted in ^{18}O enrichments in the rhyolites, not depletions. In the case of Ascension Island, where Harris (1983) showed that comenditic rhyolites were derived from some 75% basalt crystallisation, Sheppard and Harris (1985) noted that less than a 1.0‰ enrichment in ^{18}O was produced in the comendites, and concluded that O-isotope enrichments are less than 1‰ for basalt crystal fractionation up to 80%. Mechanism (*b*) would result in both degassing and superheating of the rhyolite magma, though isotopic fractionation would leave the rhyolite magma enriched rather than depleted in ^{18}O. These first two mechanisms may therefore be discounted as producing the $\delta^{18}O$ depleted rhyolites.

Mechanism (*c*) has a large body of supportive data, and has been recorded in numerous high-latitude volcanic centres (e.g. Taylor and Forester, 1971). The exact meteoric water–magma exchange mechanism is poorly characterised however, and has led some workers (Shaw, 1974; Hildreth, 1981) to question its validity. Mechanism (*d*) was considered by Sigurdsson and Sparks (1981) to be viable and, using the data of Muehlenbachs *et al.* (1974), they calculated that a combination of 65% rhyolite derived by fractional crystallisation mixed with 35% derived by fusion of ^{18}O-depleted xenoliths would produce the observed $\delta^{18}O$ variations in the rhyolites. The O data obtained for our samples (Table 4) can be used to refine these calculations slightly. A realistic pre-contamination $\delta^{18}O$ value for the rhyolites is around +2.5 to +4.0‰. Mass balance calculations reduces the *maximum* amount of xenolith component to around 26% (using −9.9 for the xenolith, +4 for the rhyolite, +0.4 for the most depleted rhyolite). The likely range is therefore between 0 and 26%.

As noted earlier, it is by no means certain that contamination of the rhyolites was achieved by a *melt* phase and the possibility of a selective contamination process (which could have involved the oxygen isotopes) is explored below. It is likely, though, that the 1875 Askja rhyolites were already ^{18}O depleted prior to their suspected contamination by the xenolithic component. The ^{18}O-depleted nature of the Askja rhyolites is therefore interpreted to result initially from isotopic exchange with $\delta^{18}O$-depleted meteoric waters (to a value about +3 to +4‰), followed by contamination by extremely ^{18}O-depleted xenolithic material resulting from basalt magma injection (Sigvaldason, 1979; Sigurdsson and Sparks, 1981) into the basal regions of the rhyolite magma body. Such a model would be consistent with the observed oxygen *and* strontium isotopic data. The 'constant' Sr isotopic composition of the rhyolites would reflect the common Sr isotopic composition of contaminant and contaminated material, while the range of O isotopic values would reflect the combined processes of isotopic exchange *and* contamination with material of different O isotopic composition.

Discussion

We have presented evidence that is consistent with fractional crystallisation being the dominant influence on the generation of the Askja rhyolitic magma. However, certain trace elements, notably Rb and Cs, and oxygen isotope data indicate that the leucocratic xenoliths have had an influence on the genesis of the rhyolite. We emphasise that these xenoliths are abundant and often occur as centimetre-sized rounded inclusions within rhyolitic pumice fragments. There are three mechanisms that occur to us which could cause modification of the rhyolite composition.

(i) *Bulk assimilation.* Differences in major and some trace elements preclude the rhyolites being simply the consequence of bulk melting. Some individual pumice clasts show characteristics that are intermediate in composition between xenoliths and rhyolites and could represent hybrids of xenolith melt and differentiated melt, as is also suggested by the cross-trend on Fig. 10. This mechanism cannot, however, account for the two to three-fold enrichment in Rb over that expected from fractional crystallization.

(ii) *Assimilation of partial melt.* Incorporation of the partial melt from the xenoliths has the advantage that these melts are rich in SiO_2 and K_2O and are likely also to be enriched in highly incompatible trace elements, such as Rb, Th and U. We have questioned the efficiency of this mechanism, however, because of physical difficulties of

separation, but we cannot preclude a role for it on purely chemical grounds.

(iii) *Selective contamination by diffusion.* When xenoliths containing a partial melt phase are dispersed within another magma, chemical diffusion can play a major role in selectively contaminating the magma (Watson, 1982; Watson and Jurewicz, 1984). When there are large differences in chemical potential of an element between magma and xenolith partial melt, and when the elements have high mobility (i.e. large diffusion coefficients), the contamination can be highly selective. Watson (1982) has carried out both experiments and theoretical calculations on this process and has concluded that the alkali elements will be particularly susceptible due to their high diffusivities compared to other elements.

This mechanism may well be applicable to the Askja case. If the xenoliths were 5 to 50 cm in diameter, a transient equilibrium could have occurred between magma and xenolith partial melt in periods of weeks to years (Watson, 1982). If the xenoliths were abundant and their partial melts were enriched in elements like Rb (and Th and U?) then the Askja rhyolite could be significantly enriched in these elements, as is observed. The process could also have worked in the opposite sense. For example if the xenolith partial melts were on average depleted in Cs compared to the rhyolite, this element would have diffused into the xenoliths and thus depleted the rhyolite in Cs. We see the relatively low Cs abundances as a fingerprint of the role of the leucocratic xenoliths in rhyolite genesis, the positive correlation between O^{18} depletion and Cs depletion (relative to Rb) marking an increasing xenolithic component (Fig. 13), and related to hydrothermal alteration.

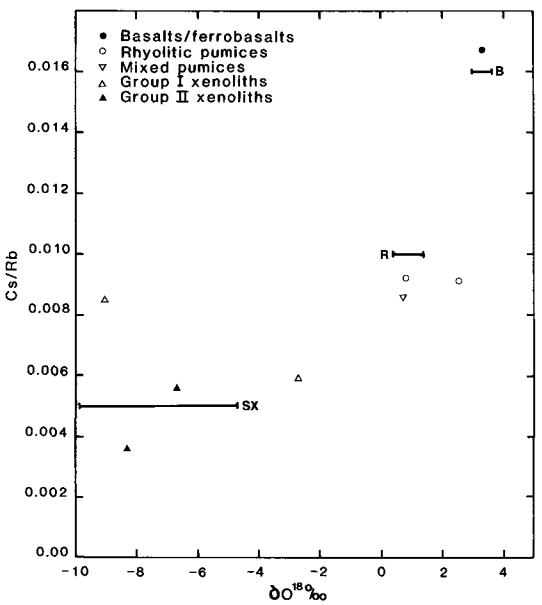

FIG. 13. Cs/Rb–$\delta^{18}O$ plot, showing the relationship between relative Cs depletion and low $\delta^{18}O$ values in the Askja rocks. The bars marked B, R and SX represent the ranges of oxygen isotope values for basalts, rhyolites and silicic xenoliths, respectively, obtained by Muehlenbachs *et al.* (1974), placed at arbitrary Cs/Rb values.

Figure 14, based on Sigurdsson and Sparks (1981, Fig. 16*a*), summarises our slightly revised ideas on the magma relationships just prior to the 1875 eruption. The relative volumes of the magma layers remain speculative since eruption processes can be highly selective in erupting zoned systems but the trace element modelling provides the following estimates. The ferrobasalts represent the residual liquids after 60–70% crystallisation of the parental, magnesian basalts. A further 50–60% crystallisation of the ferrobasalts produced the icelandites. The rhyolites were formed by about 50% crystallisation of the icelandites, and thus represent the residual liquids after 90–95% crystallisation of the basalts.

Certain aspects of the model may be elaborated.

1. The Group I and II leucocratic xenoliths are taken to have been torn from the carapace during the eruption, having been partially fused in some cases. The xenoliths represent earlier batches of silicic magma which apparently were not vented to the surface.

2. A pre-eruptive compositional zonation existed within the rhyolites in the upper part of the chamber. Chemical variations are consistent with the zonation having been derived by a combination of fractional crystallisation and selective contamination from the partially fused xenoliths.

3. An icelandite layer, of poorly known dimensions, separated the silicic and mafic parts of the system. The possibility cannot be ruled out that there existed a continuous zoning from ferrobasalt to icelandite, as in the products of Hekla (Larsen and Thorarinsson, 1977), The gap between ferrobasalt and icelandite implied by the chemical data is not well established. The scarcity of compositions between the icelandites and the most Fe-rich rhyolitic *liquids* is perhaps real in that such compositional gaps, while not fully explained yet, are common in small to medium volume systems (Smith, 1979; Hildreth, 1981). An important observation to the eventual understanding of the significance of the gaps is that the Askja icelandites were liquids. The crystal-rich character represents quenching of icelandite liquid against cooler rhyo-

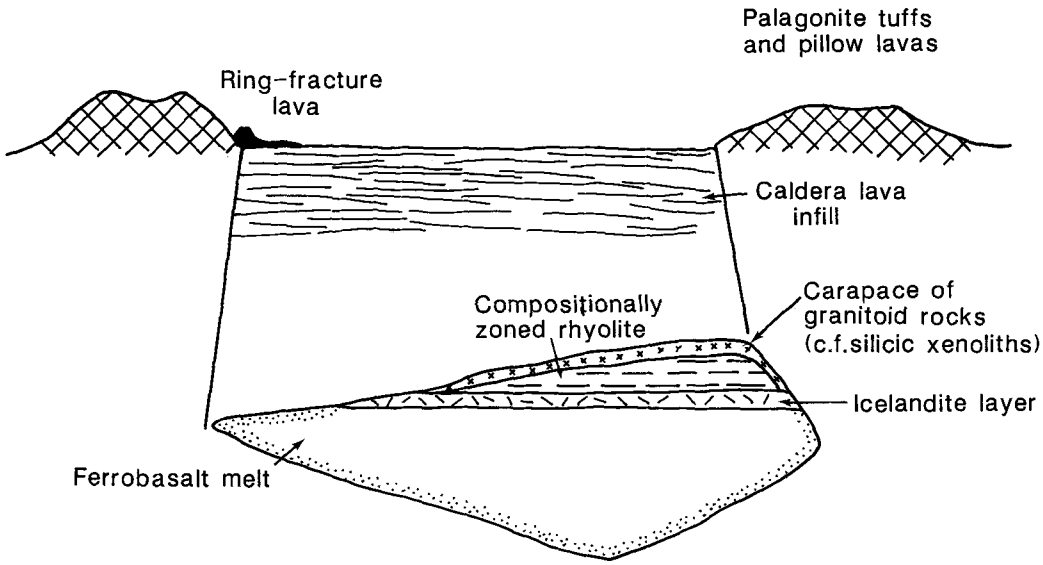

FIG. 14. A model of the Askja chamber prior to the 1875 eruption, based on Sigurdsson and Sparks (1981, Fig. 16*a*).

lite during magma mixing (Sigurdsson and Sparks, 1981).

4. Density considerations (Sigurdsson and Sparks, 1981) require that the lower part of the chamber was filled with ferrobasalt.

5. The complete compositional range was established during 1874–75. Influx of new tholeiitic basalt from depth triggered convective mixing and hybridization in the already zoned magma chamber (Sigurdsson and Sparks, 1981).

Acknowledgements

We thank J. O. Bowman and K. S. Waterhouse (University of Lancaster), and E. Y. Campbell and P. A. Baedecker (U.S. Geological Survey, Reston) for analytical assistance, C. J. Hawkesworth for arranging isotope facilities at the Open University, Peter S. Meyer (Woods Hole Oceanographic Institution) for detailed comments on the manuscript. Field work at Askja (H.S. and R.S.J.S.) was in part funded by the National Science Foundation and by Royal Society Scientific Expeditions Fund. R.S.J.S. acknowledges support by the B.P. Venture Research Fund.

References

Arth, J. G. (1976) *J. Res. U.S. Geol. Surv.* **4,** 41–7.

Bacon, C. R., Macdonald, R., Smith, R. L., and Baedecker, P. A. (1981) *J. Geophys. Res.* **86,** 10223–41.

Benjamin, T., Heuser, W. R., and Burnett, D. S. (1978) *Proc. Lunar Planet. Sci. Conf. 9th*, 1393–406.

———————and Seitz, M. G. (1980) *Geochim. Cosmochim. Acta* **44,** 1251–64.

Borthwick, J. and Harmon, R. S. (1982) Ibid. **46,** 1665–8.

Carlson, C. W., Lugmair, G. W., and MacDougall, J. D. (1981) Ibid. **45,** 2483–99.

Carmichael, I. S. E. (1964) *J. Petrol.* **5,** 435–60.

Clague, D. A. and Frey, F. A. (1982) Ibid. **23,** 447–504.

Condomines, M., Grönvold, K., Hooker, P. J., Muehlenbachs, K., O'Nions, R. K., Oskarsson, N., and Oxburgh, E. R. (1983) *Earth Planet. Sci. Lett.* **66,** 125–36.

Cox, K. G. and Hawkesworth, C. J. (1985) *J. Petrol.* **26,** 355–77.

Epstein, S., Sharp, R. P., and Gow, A. J. (1970) *Science* **168,** 1570–2.

Garlick, G. D., Macgregor, I. D., and Vogel, D. E. (1971) Ibid. **172,** 1025–7.

Gottfried, D., Greenland, L. P., and Campbell, E. Y. (1968) *Geochim. Cosmochim. Acta* **32,** 925–47.

Harris, C. (1983) *J. Petrol.* **24,** 424–70.

Hattori, K. and Muehlenbachs, K. (1982) *J. Geophys. Res.* **87,** 6559–65.

Henderson, P. (1982) *Inorganic Geochemistry.* Oxford, Pergamon, 353 pp.

Hildreth, W. (1981) *J. Geophys. Res.* **86,** 10153–92.

Irvine, T. N. and Baragar, W. R. A. (1971) *Can. J. Earth Sci.* **8,** 523–48.

Irving, A. J. (1978) *Geochim. Cosmochim. Acta* **42,** 743–70.

Larsen, G. and Thorarinsson, S. (1977) *Jokull* **27,** 28–46.

Macdonald, R., Smith, R. L., and Thomas, J. E. (in prep.) *U.S. Geol. Surv. Prof. Paper.*

Muehlenbachs, K. (1973) *Carnegie Inst. Wash. Yearb.* **72,** 593–7.

——and Byerly, G. (1982) *Contrib. Mineral. Petrol.* **79,** 76–9.

——Anderson, A. T., and Sigvaldason, G. E. (1974) *Geochim. Cosmochim. Acta.* **38,** 577–88.

Nakamura, N. (1974) Ibid. **38,** 757–75.
Norry, M. J. and Fitton, J. G. (1983) In *Continental Basalts and Mantle Xenoliths* (C. J. Hawkesworth and M. J. Norry, eds.) Shiva Publishing, 5–19.
Oskarsson, N., Sigvaldason, G. E., and Steinthorsson, S. (1982) *J. Petrol.* **23,** 28–74.
—— (1985) *J. Geophys. Res.* **90,** 10011–25.
Pearce, J. A. (1982) In *Andesites* (R. S. Thorpe, ed.) John Wiley and Sons, 525–48.
Schock, H. H. (1979) *Chem. Geol.* **26,** 119–33.
Shaw, H. R. (1974) In *Geochemical Transport and Kinetics.* Carnegie Inst. Wash. 139–70.
Sheppard, S. M. F. (1977) In *Volcanic Processes in Ore Genesis.* Inst. Mining Metallurgy and Geol. Lond. 25–41.
—— and Harris, C. (1985) *Contrib. Mineral. Petrol.* **91,** 74–81.
Sigurdsson, H. (1970) Ph.D. thesis, University of Durham.
—— and Sparks, R. S. J. (1978) *Bull. Volcan.* **41,** 149–67.
———— (1981) *J. Petrol.* **22,** 41–84.
Sigvaldason, G. E. (1974) Ibid. **15,** 497–524.
—— (1979) *Nordic Volcanol. Inst. Report 03,* Reykjavik.
Smith, R. L. (1979) Geol. Soc. Am. Spec. Pap. **180,** 5–27.
Sparks, R. S. J., Sigurdsson, H., and Wilson, L. (1977) *Nature* **267,** 315–8.
—— Wilson, L., and Sigurdsson, H. (1981) *Phil. Trans. R. Soc. Lond.* A**299,** 241–73.
Sun, S-S. and Hanson, G. N. (1976) *Contrib. Mineral. Petrol.* **54,** 139–55.
Taylor, H. P., Jr. (1968) Ibid. **19,** 1–71.
—— and Epstein, S. (1962) *Bull. Geol. Soc. Am.* **73,** 461–80.
—— and Forester, R. W. (1971) *J. Petrol.* **12,** 465–97.
Thirlwall, M. F. and Jones, N. W. (1983) *Continental Basalts and Mantle Xenoliths* (C. J. Hawkesworth and M. J. Norry, eds.) Shiva Publishing, 186–208.
Thompson, R. N. (1982) *Scott. J. Geol.* **18,** 49–107.
—— Dickin, A. P., Gibson, I. L., and Morrison, M. A. (1982) *Contrib. Mineral. Petrol.* **79,** 159–68.
Watson, E. B. (1982) Ibid. **80,** 73–87.
—— and Jurewicz, S. R. (1984) *J. Geol.* **92,** 121–31.
Wood, D. A. (1978) *J. Petrol.* **19,** 393–436.
—— Joron, J-L., Treuil, M., Norry, M., and Tarney, J. (1979) *Contrib. Mineral. Petrol.* **70,** 319–39.
Zindler, A., Jagoutz, E., and Goldstein, A. (1982) *Nature,* **298,** 519–23.
—— Staudigel, H., and Batiza, R. (1984) *Earth Planet. Sci. Lett.* **70,** 175–95.

[*Manuscript received 29 March 1984; revised 27 June 1986*]